FDTD Modeling of Dispersive Bianisotropic Media Using Z-Transform Method

Vahid Nayyeri, *Student Member, IEEE*, Mohammad Soleimani, Jalil Rashed-Mohassel, *Senior Member, IEEE*, and Mojtaba Dehmollaian

Abstract—The finite-difference time-domain (FDTD) technique for simulating electromagnetic wave interaction with a dispersive chiral medium is extended to include the simulation of dispersive bianisotropic media. Due to anisotropy and frequency dispersion of such media, the constitutive parameters are represented by frequency-dependent tensors. The FDTD is formulated using the Z-transform method, a conventional approach for applying FDTD in frequency-dispersive media. Omega medium is considered as an example of bianisotropic media, the frequency-dependent tensors of which are based on analytical models. The extended FDTD method is used to determine the reflection and transmission coefficients of co- and cross-polarized electromagnetic waves from omega slabs, illuminated by normally incident plane waves. Three cases are simulated: 1) a slab of uniaxial omega medium with its optical axis parallel to the propagation vector; 2) a slab of rotated uniaxial omega medium with its optical axis not parallel to the propagation vector; and 3) a slab of biaxial omega medium. The results are validated by means of comparisons with analytical solutions.

Index Terms—Bianisotropic media, chiral medium, dispersive media, finite-difference time-domain (FDTD), omega medium, Z-transform method.

I. INTRODUCTION

A rapidly growing research interest in the field of electromagnetics is the physical and electromagnetic (EM) properties of materials. Due to the need for special EM properties, artificially structured metamaterials, such as bimedia, classified as materials exhibiting magnetoelectric coupling, are suggested.

Bimedia are investigated for various applications such as antenna radomes [1], [2], waveguides [3]–[5] and polarization transformers [6]. They are also studied for substrates of microstrip antennas [7]–[10], absorbers [11], [12], backward wave media [13], and cloaking materials [14].

In these materials, there is a coupling between electric and magnetic fields which causes simultaneous production of electric and magnetic polarizations due to the electric or magnetic excitation. This phenomenon is mathematically represented by magnetoelectric coupling tensors or coefficients in constitutive relations which make electric and magnetic flux densities dependent on both electric and magnetic fields.

Bimedia themselves are divided into biisotropic and bianisotropic subclasses. The properties of the former are not dependent on the direction; so its constitutive parameters are scalars. However, the latter, which exhibits different behaviors in different directions, has tensor constitutive parameters. Chiral and pseudochiral omega materials are samples of biisotropic and bianisotropic media, respectively.

Modeling EM wave interaction with bimedia is an important problem, which has been investigated analytically and numerically. Finite-difference time-domain (FDTD) is one of the numerical methods used for modeling chiral media as well as biisotropic media. FDTD modeling of biisotropic media is studied in different articles [15]–[25], in some of which the effects of frequency dispersion are accounted for [20]–[25].

Many approaches are introduced for modeling dispersive media using FDTD method. Several summaries of various methods are given in [26]–[28]. Among them, the auxiliary differential equation (ADE), the Z-transform, and the piecewise linear recursive convolution (PLRC) approaches are widely used and proven to be very accurate. Comparisons of their accuracy and stability, given in [29] for Lorentz media, show that the stability limits of these approaches are approximately the same. However, the Z-transform approach has the best accuracy near resonant frequencies and is very easy to implement.

Demir *et al.* [22] studied FDTD modeling of chiral media using the Z-transform method. They incorporated the dispersive nature of permittivity, permeability and chirality in the FDTD formulation and provided a full dispersive model in which frequency dependence of permittivity and permeability follows the Lorentz model and that frequency dependence of chirality follows the Condon model. Their work is based on converting frequency domain constitutive relations to Z-domain relations, proper forms for deriving FDTD updating equations. In this transform, backward time differences are used for time derivatives in order to decouple updating equations for electric and magnetic field components. Another FDTD model of dispersive chiral media using transformation to Z domain was developed by Pereda *et al.* [25]. In [25], Maxwell's curl equations, firstly expressed in Laplace domain, are directly transformed to discrete-time domain. On the other hand, the constitutive relations, also expressed in Laplace domain, are first converted to Z domain using Mobius transform [30]; they are then expressed in the discrete-time domain. In this method, central differences are

used for time derivatives to preserve the second-order accuracy of the conventional FDTD.

Furthermore, Akyurtlu *et al.* introduced a FDTD method for modeling transverse propagation through a uniaxial bianisotropic medium [31] called BA-FDTD. This method is based on decomposing electric and magnetic fields into the $\pm$ wave-fields. They treated the anisotropic chiral medium problem as the sum of two problems associated with non-chiral anisotropic media. In their simulation, an axially chiral medium as a bianisotropic medium with no frequency dispersion is considered.

Furthermore, omega medium is a bianisotropic medium formed by including Ω-shaped metal elements inside an isotropic dielectric material. This medium is suggested by Saadun and called pseudochiral Ω medium [32]. When an external electric (or magnetic) field is applied to an omega particle, it induces an electric dipole moment parallel to its stem and a magnetic moment orthogonal to its loop. This causes magnetoelectric coupling in the medium. As mentioned before, the constitutive parameters of this medium are frequency dependent tensors. Several papers have introduced a number of reliable analytical models of Ω particles and omega medium which have been developed and validated numerically and experimentally [33]–[35].

In the present paper, the FDTD formulation for dispersive chiral media using the Z-transform method [22], simply implementable and well accurate, is extended in order to include a more general case of bianisotropic media. Omega medium is assumed as an example of bianisotropic media whose frequency dispersion model follows the forms given in [13], based on the analytical models. In Section II, the theoretical development of the FDTD formulation in dispersive bianisotropic media is presented. Finally, in Section III, the presented FDTD formulation is validated by simulating the interaction of a plane wave with an omega slab in three cases of uniaxial omega slab, rotated uniaxial omega slab, and rotated biaxial omega slab. The analytical solution method, given in [36], is used for validating the results.

II. Theoretical Development

In this section, the basic theory of FDTD formulation for dispersive bianisotropic media is presented in two parts. Since constitutive relations of media are used in deriving FDTD updating equations, the constitutive properties of the media are described in part A. These relations are considered in the forms suggested by [37] for uniaxial and biaxial cases. Next, an omega medium is studied as a sample of bianisotropic media. The frequency dispersion models of this medium are taken from [13]. Finally, the effect of axes rotations of the medium is investigated. In part B, the FDTD formulation for dispersive bianisotropic media, discussed in part A, is explained using the Z-transform method.

A. Constitutive Relations and Frequency Models

Bianisotropic media are classified as media with two properties, anisotropy and magnetoelectric coupling.

A bianisotropic medium can be made by including small metal particles with loops and handles (like Ω) embedded in a dielectric host medium. The resonant behavior of particles leads to the frequency dispersion of the medium which makes the constitutive parameters frequency dependent. One type of such
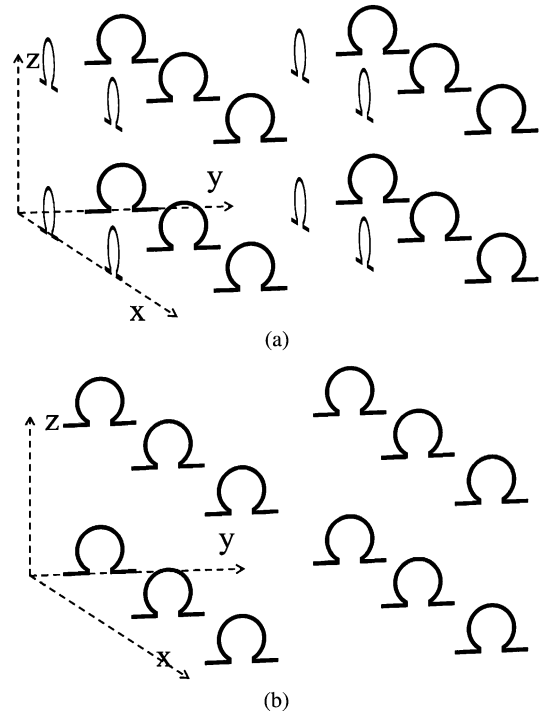

Fig. 1. Geometry of the omega structure: (a) a uniaxial medium with optical axis along $\hat{z}$ direction. (b) A biaxial medium.

materials is a pseudochiral Ω medium (omega medium) that can be realized as a composite with Ω-shaped metal inclusions, shown in Fig. 1. In Fig. 1(a), Ω-shaped metal elements lie in planes parallel to xz- and yz-planes (i.e., uniaxial medium) and, in Fig. 1(b), all of these elements lie in planes parallel to yz-plane (i.e., biaxial medium). Generally, the constitutive relations in a reciprocal bianisotropic medium in frequency domain can be written as [37]

$$\overline{D}(\omega) = \overline{\overline{\varepsilon}}(\omega).\overline{E}(\omega) + \overline{\overline{\alpha}}(\omega).\overline{H}(\omega) \tag{1.a}$$

$$\overline{B}(\omega) = \overline{\overline{\mu}}(\omega)\overline{H}(\omega) - \overline{\overline{\alpha}}^{t}(\omega).\overline{E}(\omega) \tag{1.b}$$

where $\overline{E}, \overline{D}, \overline{H}$, and $\overline{B}$ are the electric field, electric flux density, magnetic field, and magnetic flux density, respectively. In (1), $\overline{\overline{\varepsilon}}$, $\overline{\overline{\mu}}$, and $\overline{\overline{\alpha}}$ present permittivity, permeability, and magnetoelectric coupling frequency-dependent tensors, respectively. The superscript t stands for transpose. It is noted that due to anisotropy of the medium, the constitutive parameters are in tensor forms and, because of frequency dispersion, they are frequency dependent. In the following, constitutive relations of two cases (uniaxial and biaxial) of bianisotropic media are reviewed.

According to Fig. 1(a), in a uniaxial bianisotropic medium in which the optical axis is along $\hat{z}$, the constitutive tensors are given by

$$\overline{\overline{\varepsilon}}(\omega) = \varepsilon_0 \left(\varepsilon_t(\omega)\overline{\overline{I}}_t + \varepsilon_n(\omega)\hat{z}\hat{z} \right) \tag{2.a}$$

$$\overline{\overline{\mu}}(\omega) = \mu_0 \left(\mu_t(\omega)\overline{\overline{I}}_t + \mu_n(\omega)\hat{z}\hat{z} \right) \tag{2.b}$$

$$\overline{\overline{\alpha}}(\omega) = j\sqrt{\varepsilon_0\mu_0}K(\omega)\overline{\overline{J}} \tag{2.c}$$

where $\overline{\overline{I}}_t = \overline{\overline{I}} - \hat{z}\hat{z} = \hat{x}\hat{x} + \hat{y}\hat{y}$ and $\overline{\overline{J}} = \hat{z} \times \overline{\overline{I}} = \hat{y}\hat{x} - \hat{x}\hat{y}$ are the two-dimensional (2-D) transverse symmetric and antisymmetric

unit dyads defined in the xy-plane, respectively. Here, subscript t stands for transverse. Also, in (2.c), K is a complex dimensionless parameter that measures the magnetoelectric coupling effect. Substituting (2) in (1) and considering $\overline{\overline{J}} = -\overline{\overline{J}}^t$, the constitutive relations in a uniaxial bianisotropic medium with optical axis along $\hat{z}$ are determined by

$$\overline{D} = \varepsilon_0 \left(\varepsilon_t(\omega)\overline{\overline{I}}_t + \varepsilon_n(\omega)\hat{z}\hat{z} \right).\overline{E} + j\sqrt{\varepsilon_0\mu_0}K(\omega)\overline{\overline{J}}.\overline{H} \quad (3.a)$$

$$\overline{B} = \mu_0 \left(\mu_t(\omega)\overline{\overline{I}}_t + \mu_n(\omega)\hat{z}\hat{z} \right).\overline{H} + j\sqrt{\varepsilon_0\mu_0}K(\omega)\overline{\overline{J}}.\overline{E}. \quad (3.b)$$

Moreover, in a biaxial bianisotropic medium, as shown in Fig. 1(b), the constitutive tensors are given by

$$\overline{\overline{\varepsilon}} = \varepsilon_0 \left(\varepsilon_t(\omega)\hat{y}\hat{y} + \varepsilon_n(\omega)\left(\hat{x}\hat{x} + \hat{z}\hat{z}\right) \right) \quad (4.a)$$

$$\overline{\overline{\mu}} = \mu_0 \left(\mu_t(\omega)\hat{x}\hat{x} + \mu_n(\omega)\left(\hat{y}\hat{y} + \hat{z}\hat{z}\right) \right) \quad (4.b)$$

$$\overline{\overline{\alpha}}(\omega) = j\sqrt{\varepsilon_0\mu_0}K(\omega)\hat{y}\hat{x}. \quad (4.c)$$

The constitutive relations of this medium are obtained by substituting (4) in (1).

$$\overline{D} = \varepsilon_0 \left(\varepsilon_t(\omega)\hat{y}\hat{y} + \varepsilon_n(\omega)\left(\hat{x}\hat{x} + \hat{z}\hat{z}\right) \right).\overline{E}$$
$$+ j\sqrt{\varepsilon_0\mu_0}K(\omega)\hat{y}\hat{x}.\overline{H} \quad (5.a)$$

$$\overline{B} = \mu_0 \left(\mu_t(\omega)\hat{x}\hat{x} + \mu_n(\omega)\left(\hat{y}\hat{y} + \hat{z}\hat{z}\right) \right).\overline{H}$$
$$- j\sqrt{\varepsilon_0\mu_0}K(\omega)\hat{x}\hat{y}.\overline{E}. \quad (5.b)$$

Considering an omega medium as a bianisotropic medium and assuming the quasi-static polarization of Ω particles in the z-direction, the dispersion of relative normal permittivity, ε_n, and permeability, μ_n, can be neglected [33]. The relative transversal permittivity, ε_t, relative transversal permeability, μ_t, and magnetoelectric coupling, K, assuming low-density of Ω particles, are given by [13]

$$\varepsilon_t(\omega) = \varepsilon_\infty + \frac{(\varepsilon_s - \varepsilon_\infty)\omega_0^2}{\omega_0^2 - \omega^2 + j2\omega_0\xi_0\omega} \quad (6.a)$$

$$\mu_t(\omega) = \mu_s + \frac{(\mu_s - \mu_\infty)\omega^2}{\omega_0^2 - \omega^2 + j2\omega_0\xi_0\omega} \quad (6.b)$$

$$K(\omega) = \frac{\tau_K\omega_0^2\omega}{\omega_0^2 - \omega^2 + j2\omega_0\xi_0\omega} \quad (6.c)$$

where ω_0, ξ_0, and τ_K are resonant frequency, damping ratio, and magnetoelectric coupling coefficient, respectively. In (6), ε_s and μ_s are static relative permittivity and permeability, and ε_∞ and μ_∞ are relative permittivity and permeability at frequencies much larger than ω_0, respectively.

If the coordinate axes rotate by Euler angles α, β, and γ, the constitutive tensors of the medium with respect to the rotated coordinates, $\overline{\overline{\varepsilon}}_{rotated}$, $\overline{\overline{\mu}}_{rotated}$, and $\overline{\overline{\alpha}}_{rotated}$ can be calculated through

$$\overline{\overline{\varepsilon}}_{rotated} = U^t\overline{\overline{\varepsilon}}U \quad (7.a)$$

$$\overline{\overline{\mu}}_{rotated} = U^t\overline{\overline{\mu}}U \quad (7.b)$$

$$\overline{\overline{\alpha}}_{rotated} = U^t\overline{\overline{\alpha}}U \quad (7.c)$$

where $\overline{\overline{\varepsilon}}$, $\overline{\overline{\mu}}$, and $\overline{\overline{\alpha}}$ are parameters, given in (2) and (4) for uniaxial and biaxial media, respectively. In (7), U is the rotation matrix defined by

$$U = \begin{bmatrix} \cos\alpha & -\sin\alpha & 0 \\ \sin\alpha & \cos\alpha & 0 \\ 0 & 0 & 1 \end{bmatrix} \times \begin{bmatrix} 1 & 0 & 0 \\ 0 & \cos\beta & -\sin\beta \\ 0 & \sin\beta & \cos\beta \end{bmatrix}$$
$$\times \begin{bmatrix} \cos\gamma & -\sin\gamma & 0 \\ \sin\gamma & \cos\gamma & 0 \\ 0 & 0 & 1 \end{bmatrix} \quad (8)$$

where α, β, and γ are Euler angles [38].

Substituting (4) and (2) in (7), the constitutive tensors of rotated uniaxial and biaxial bianisotropic media are calculated by (9) and (10), respectively, as follows:

$$\overline{\overline{\varepsilon}}(\omega) = \varepsilon_0 U^t \left(\varepsilon_t(\omega)\overline{\overline{I}}_t + \varepsilon_n\hat{z}\hat{z} \right) U \quad (9.a)$$

$$\overline{\overline{\mu}}(\omega) = \mu_0 U^t \left(\mu_t(\omega)\overline{\overline{I}}_t + \mu_n\hat{z}\hat{z} \right) U \quad (9.b)$$

$$\overline{\overline{\alpha}}(\omega) = j\sqrt{\varepsilon_0\mu_0}K(\omega)U^t.\overline{\overline{J}}.U \quad (9.c)$$

$$\overline{\overline{\varepsilon}} = \varepsilon_0 U^t(\varepsilon_t\hat{y}\hat{y} + \varepsilon_n\hat{x}\hat{x} + \varepsilon_n\hat{z}\hat{z})U \quad (10.a)$$

$$\overline{\overline{\mu}} = \mu_0 U^t(\mu_t\hat{x}\hat{x} + \mu_n\hat{y}\hat{y} + \mu_n\hat{z}\hat{z})U \quad (10.b)$$

$$\overline{\overline{\alpha}} = j\sqrt{\varepsilon_0\mu_0}KU^t.\hat{y}\hat{x}.U. \quad (10.c)$$

In the following subsection, the extension of FDTD method for simulating the wave interaction with dispersive bianisotropic media is presented.

B. FDTD Formulation of Dispersive Bianisotropic Media

Basically, the FDTD method is based on simultaneous solutions of Maxwell's curl equations in the time domain

$$\nabla \times \overline{H} = \frac{\partial\overline{D}}{\partial t} \quad (11.a)$$

$$\nabla \times \overline{E} = -\frac{\partial\overline{B}}{\partial t}. \quad (11.b)$$

Two major tasks are taken in a simple FDTD formulation of a dispersive medium: first, updating flux densities $\overline{D}$ and $\overline{B}$ by decomposing and discretizing the curl equations in time and space, and second, deriving equations in order to update fields $\overline{E}$ and $\overline{H}$ using constitutive relations.

In the first step, updating equations for $\overline{D}$ and $\overline{B}$ are formed by decomposing (11) into x, y, and z components and discretizing them in time and space. For example, for the component x, we have

$$D_x^{n+1}\left(i + \frac{1}{2}, j, k\right)$$
$$= D_x^n\left(i + \frac{1}{2}, j, k\right)$$
$$+ \frac{\Delta t}{\Delta y}\left[H_z^{n+\frac{1}{2}}\left(i + \frac{1}{2}, j + \frac{1}{2}, k\right)\right.$$
$$\left. - H_z^{n+\frac{1}{2}}\left(i + \frac{1}{2}, j - \frac{1}{2}, k\right)\right]$$

$$-\frac{\Delta t}{\Delta z}\left[H_y^{n+\frac{1}{2}}\left(i+\frac{1}{2},j,k+\frac{1}{2}\right)\right.$$

$$\left.-H_y^{n+\frac{1}{2}}\left(i+\frac{1}{2},j,k-\frac{1}{2}\right)\right] \quad (12.a)$$

$$B_x^{n+1}\left(i,j+\frac{1}{2},k+\frac{1}{2}\right)$$

$$=B_x^n\left(i,j+\frac{1}{2},k+\frac{1}{2}\right)$$

$$-\frac{\Delta t}{\Delta y}\left[E_z^{n+\frac{1}{2}}\left(i,j+1,k+\frac{1}{2}\right)\right.$$

$$\left.-E_z^{n+\frac{1}{2}}\left(i,j,k+\frac{1}{2}\right)\right]$$

$$+\frac{\Delta t}{\Delta z}\left[E_y^{n+\frac{1}{2}}\left(i,j+\frac{1}{2},k+1\right)\right.$$

$$\left.-E_y^{n+\frac{1}{2}}\left(i,j+\frac{1}{2},k\right)\right]. \quad (12.b)$$

Components y and z can also be obtained in a similar way.

In the second step, the updating equations for field values are derived using constitutive relations given in the frequency domain (1). Since the updating equations are time-domain relations, the frequency-domain constitutive relations (1) may be converted to the time-domain ones. This transformation involves convolution integrals. To avoid the time consuming computation of convolutions, the constitutive relations are expressed in Z domain as follows:

$$\overline{D}(z)=\overline{\overline{\varepsilon}}(z).\overline{E}(z)T+\sqrt{\varepsilon_0\mu_0}\overline{\overline{\alpha}}(z).\overline{H}(z)T \quad (13.a)$$

$$\overline{B}(z)=\overline{\overline{\mu}}(z).\overline{H}(z)T-\sqrt{\varepsilon_0\mu_0}\overline{\overline{\alpha}}^T(z).\overline{E}(z)T \quad (13.b)$$

where T is the sampling period of time discretization in Z transform, and $\overline{\overline{\varepsilon}}(z)$, $\overline{\overline{\mu}}(z)$, and $\overline{\overline{\alpha}}(z)$ are the Z transforms of the time-domain tensors whose Fourier transforms are $\overline{\overline{\varepsilon}}(\omega)$, $\overline{\overline{\varepsilon}}(\omega)$, and $\overline{\overline{\alpha}}(\omega)$, respectively. The main advantage of using Z transform is that multiplications in the frequency domain are preserved in the Z domain. This approach is suggested by Sullivan as "Z-transform method" for FDTD modeling of wave propagation in dispersive media [39]. In this method, determining constitutive parameters in the Z domain is required. If the Z-domain constitutive parameters are expressed in the form of

$$\frac{\sum_{i=1}^{M}b_iz^{-i}}{\sum_{i=1}^{N}a_iz^{-i}}$$

where a_i, b_i, N, and M are constants and $N\geq M$, then $\overline{E}(z)$ and $\overline{H}(z)$ are simply expressed by polynomials of order z^{-N}. It is noticed that since $z^{-n}F(z)$ in the Z domain is equivalent to $f(t-nT)$ in the time domain, a simple updating algorithm is obtained.

Given constitutive tensors in bianisotropic medium (9) and (10) and their frequency-dependent components (6), the task is to evaluate $\overline{\overline{\varepsilon}}(z)$, $\overline{\overline{\mu}}(z)$, and $\overline{\overline{\alpha}}(z)$. First, by separating the fre-

quency-dependent parts from the independent parts, the followings are concluded

$$\overline{D}(\omega)=\left(\overline{\overline{\varepsilon^c}}+\overline{\overline{\varepsilon^\omega}}(\omega)\right).\overline{E}(\omega)+j\sqrt{\varepsilon_0\mu_0}\overline{\overline{\alpha}}(\omega).\overline{H}(\omega) \quad (14.a)$$

$$\overline{B}(\omega)=\left(\overline{\overline{\mu^c}}+\overline{\overline{\mu^\omega}}(\omega)\right).\overline{H}(\omega)+j\sqrt{\varepsilon_0\mu_0}\overline{\overline{\alpha}}^t(\omega).\overline{E}(\omega) \quad (14.b)$$

where $\overline{\overline{\varepsilon^c}}$, $\overline{\overline{\varepsilon^\omega}}(\omega)$, $\overline{\overline{\mu^c}}$, $\overline{\overline{\mu^\omega}}(\omega)$, and $\overline{\overline{\alpha}}(\omega)$ are given by

$$\overline{\overline{\varepsilon^c}}=\varepsilon_\infty\overline{\overline{\mathrm{M}}}_e+\varepsilon_n\overline{\overline{\mathrm{N}}}_e \quad (15.a)$$

$$\overline{\overline{\varepsilon^\omega}}(\omega)=\frac{(\varepsilon_s-\varepsilon_\infty)\omega_\varepsilon^2}{\omega_\varepsilon^2-\omega^2+j2\omega_\varepsilon\xi_\varepsilon\omega}\overline{\overline{\mathrm{M}}}_e \quad (15.b)$$

$$\overline{\overline{\mu^c}}=\mu_s\overline{\overline{\mathrm{M}}}_m+\mu_n\overline{\overline{\mathrm{N}}}_m \quad (15.c)$$

$$\overline{\overline{\mu^\omega}}(\omega)=\frac{(\mu_\infty-\mu_s)\omega^2}{\omega_0^2-\omega^2+j2\omega_0\xi_0\omega}\overline{\overline{\mathrm{M}}}_m \quad (15.d)$$

$$\overline{\overline{\alpha}}(\omega)=j\sqrt{\varepsilon_0\mu_0}K(\omega)\overline{\overline{\mathrm{O}}}. \quad (15.e)$$

In (15), $\overline{\overline{\mathrm{M}}}_e=\overline{\overline{\mathrm{M}}}_m=\overline{\overline{U}}^t\overline{\overline{I}}_t\overline{\overline{U}}$, $\overline{\overline{\mathrm{N}}}_e=\overline{\overline{\mathrm{N}}}_m=\overline{\overline{U}}^t\hat{z}\hat{z}\overline{\overline{U}}$, and $\overline{\overline{\mathrm{O}}}=\overline{\overline{U}}^t\overline{\overline{JU}}$ in the uniaxial case, shown in Fig. 1(a) and $\overline{\overline{\mathrm{M}}}_e=\overline{\overline{U}}^t\hat{y}\hat{y}\overline{\overline{U}}$, $\overline{\overline{\mathrm{N}}}_e=\overline{\overline{U}}^t(\hat{x}\hat{x}+\hat{z}\hat{z})\overline{\overline{U}}$, $\overline{\overline{\mathrm{M}}}_m=\overline{\overline{U}}^t\hat{x}\hat{x}\overline{\overline{U}}$, $\overline{\overline{\mathrm{N}}}_m=\overline{\overline{U}}^t(\hat{y}\hat{y}+\hat{z}\hat{z})\overline{\overline{U}}$, and $\overline{\overline{\mathrm{O}}}=\overline{\overline{U}}^t\hat{y}\hat{x}\overline{\overline{U}}$ in the biaxial case, shown in Fig. 1(b).

To convert frequency-domain relations to Z domain, the following relations are used [39]:

$$\mathrm{F}(\omega)=\frac{\beta}{(\rho^2+\beta^2)+j2\rho\omega-\omega^2}\Leftrightarrow$$

$$F(z)=\frac{\varepsilon^{-\rho T}\sin(\beta T)z^{-1}}{1-2e^{-\rho T}\cos(\beta T)\cdot z^{-1}+e^{-2\rho T}z^{-2}} \quad (16.a)$$

$$\mathrm{F}(\omega)=\beta\Leftrightarrow F(z)=\frac{\beta}{T} \quad (16.b)$$

$$j\omega\mathrm{F}(\omega)\Leftrightarrow\frac{1-z^{-1}}{T}F(z) \quad (16.c)$$

$$\omega^2\mathrm{F}(\omega)\Leftrightarrow-\left(\frac{1-z^{-1}}{T}\right)^2F(z) \quad (16.d)$$

where β and ρ are constants.

Applying these transformations to (15), the Z-domain constitutive tensors $\overline{\overline{\varepsilon}}(z)$, $\overline{\overline{\mu}}(z)$, and $\overline{\overline{\alpha}}(z)$ in (13) become (17), shown at the bottom of the next page.

The next task is to express constitutive relations in Z domain. This is obtained by substituting (17) in (13)

$$\overline{D}(z)=\left(\overline{\overline{\varepsilon^c}}+\frac{C_{\varepsilon1}z^{-1}}{1-C_{\varepsilon2}z^{-1}+C_{\varepsilon3}z^{-2}}\overline{\overline{\mathrm{M}}}_e\right).\overline{E}(z)$$

$$+\frac{C_{\alpha1}z^{-1}-C_{\alpha1}z^{-2}}{1-C_{\alpha2}z^{-1}+C_{\alpha3}z^{-2}}\overline{\overline{\mathrm{O}}}.\overline{H}(z) \quad (18.a)$$

$$\overline{B}(z)=\left(\overline{\overline{\mu^c}}+\frac{C_{\mu1}z^{-1}-2C_{\mu1}z^{-2}+C_{\mu1}z^{-3}}{1-C_{\mu2}z^{-1}+C_{\mu3}z^{-2}}\overline{\overline{\mathrm{M}}}_m\right).\overline{H}(z)$$

$$-\left(\frac{C_{\alpha1}z^{-1}-C_{\alpha1}z^{-2}}{1-C_{\alpha2}z^{-1}+C_{\alpha3}z^{-2}}\overline{\overline{\mathrm{O}}}^t\right).\overline{E}(z) \quad (18.b)$$

where

$$C_{\varepsilon1}=\frac{T(\varepsilon_s-\varepsilon_\infty)\omega_0e^{-\omega_0\xi_0T}\sin\left(\omega_0\sqrt{1-\xi_0^2}T\right)}{\sqrt{1-\xi_0^2}} \quad (19.a)$$

$$C_{\varepsilon 2} = 2e^{-\omega_0 \xi_0 T} \cos\left(\omega_0 \sqrt{1-\xi_0^2}\, T\right) \tag{19.b}$$

$$C_{\varepsilon 3} = e^{-2\omega_0 \xi_0 T} \tag{19.c}$$

$$C_{\mu 1} = \frac{(\mu_\infty - \mu_s)e^{-\omega_0 \xi_0 T} \sin\left(\omega_0 \sqrt{1-\xi_0^2}\, T\right)}{T\omega_0 \sqrt{1-\xi_0^2}} \tag{19.d}$$

$$C_{\mu 2} = 2e^{-\omega_0 \xi_0 T} \cos\left(\omega_0 \sqrt{1-\xi_0^2}\, T\right) \tag{19.e}$$

$$C_{\mu 3} = e^{-2\omega_0 \xi_0 T} \tag{19.f}$$

$$C_{\alpha 1} = \frac{\tau_\alpha \omega_0 e^{-\omega_0 \xi_0 T} \sin\left(\omega_0 \sqrt{1-\xi_0^2}\, T\right)\sqrt{\varepsilon_0 \mu_0}}{\sqrt{1-\xi_0^2}} \tag{19.g}$$

$$C_{\alpha 2} = 2e^{-\omega_0 \xi_0 T} \cos\left(\omega_0 \sqrt{1-\xi_0^2}\, T\right) \tag{19.h}$$

$$C_{\alpha 3} = e^{-2\omega_0 \xi_0 T}. \tag{19.i}$$

It is interesting to note that by separating z terms, s (18) can be written as

$$\overline{D}(z) = \overline{\overline{\varepsilon^c}} . \overline{E}(z) + \overline{S}_e(z)z^{-1}$$
$$+ \overline{S}_{\alpha h}(z)z^{-1} - \overline{S}_{\alpha h}(z)z^{-2} \tag{20.a}$$

$$\overline{B}(z) = \overline{\overline{\mu^c}} . \overline{H}(z) + \overline{S}_h(z)z^{-1} - 2\overline{S}_h(z)z^{-2}$$
$$+ \overline{S}_h(z)z^{-3} - \overline{S}_{\alpha e}(z)z^{-1} + \overline{S}_{\alpha e}(z)z^{-2} \tag{20.b}$$

where vectors $\overline{S}_e$, $\overline{S}_h$, $\overline{S}_{\alpha e}$, and $\overline{S}_{\alpha h}$ are defined as

$$\overline{S}_e(z) = \frac{C_{\varepsilon 1}}{1 - C_{\varepsilon 2}z^{-1} + C_{\varepsilon 3}z^{-2}} \overline{\overline{M}}_e . \overline{E}(z) \tag{21.a}$$

$$\overline{S}_h(z) = \frac{C_{\mu 1}}{1 - C_{\mu 2}z^{-1} + C_{\mu 3}z^{-2}} \overline{\overline{M}}_m . \overline{H}(z) \tag{21.b}$$

$$\overline{S}_{\alpha e}(z) = \frac{C_{\alpha 1}}{1 - C_{\alpha 2}z^{-1} + C_{\alpha 3}z^{-2}} \overline{\overline{O}}^t . \overline{E}(z) \tag{21.c}$$

$$\overline{S}_{\alpha h}(z) = \frac{C_{\alpha 1}}{1 - C_{\alpha 2}z^{-1} + C_{\alpha 3}z^{-2}} \overline{\overline{O}} . \overline{H}(z). \tag{21.d}$$

At this point, the Z-domain equations that yield the updating equations for field values can be simply extracted from (20) in the following way:

$$\overline{E}(z) = (\overline{\overline{\varepsilon^c}})^{-1} . \left[\overline{D}(z) - \overline{S}_e(z)z^{-1} - \overline{S}_{\alpha h}(z)z^{-1} + \overline{S}_{\alpha h}(z)z^{-2}\right] \tag{22.a}$$

$$\overline{H}(z) = (\overline{\overline{\mu^c}})^{-1} . \left[\overline{B}(z) - \overline{S}_h(z)z^{-1} + 2\overline{S}_h(z)z^{-2} - \overline{S}_h(z)z^{-3} + \overline{S}_{\alpha e}(z)z^{-1} - \overline{S}_{\alpha e}(z)z^{-2}\right]. \tag{22.b}$$

Now, the property of Z transform $Z[x[n-1]] = z^{-1}Z[x[n]]$ is used in the derivation of updating equations of fields $\overline{E}$ and $\overline{H}$. By setting the sampling period, T, equal to one-half of the time step in FDTD [39], (22) can be written as

$$\overline{E}^{n+1} = (\overline{\overline{\varepsilon^c}})^{-1} . \left[\overline{D}^{n+1} - \overline{S}_e^{n+\frac{1}{2}} - \overline{S}_{\alpha h}^{n+\frac{1}{2}} + \overline{S}_{\alpha h}^n\right] \tag{23.a}$$

$$\overline{H}^{n+1} = (\overline{\overline{\mu^c}})^{-1} . \left[\overline{B}^{n+1} - \overline{S}_h^{n+\frac{1}{2}} + 2\overline{S}_h^n - \overline{S}_h^{n-\frac{1}{2}} + \overline{S}_{\alpha e}^{n+\frac{1}{2}} - \overline{S}_{\alpha e}^n\right] \tag{23.b}$$

in discrete-time domain. Equations (23) are decomposed into x, y, and z components and used in the FDTD formulation. For example, for the x components of fields we have

$$E_x^{n+1}\left(i+\frac{1}{2}, j, k\right)$$
$$= +(\overline{\overline{\varepsilon^c}})_{11}^{-1}\left[D_x^{n+1}\left(i+\frac{1}{2}, j, k\right) - S_{e,x}^{n+\frac{1}{2}}\left(i+\frac{1}{2}, j, k\right)\right.$$
$$\left. + S_{\alpha h,x}^{n+\frac{1}{2}}\left(i+\frac{1}{2}, j, k\right) - S_{\alpha h,x}^n\left(i+\frac{1}{2}, j, k\right)\right]$$
$$+(\overline{\overline{\varepsilon^c}})_{12}^{-1}\left[D_y^{n+1}\left(i+\frac{1}{2}, j, k\right) - S_{e,y}^{n+\frac{1}{2}}\left(i+\frac{1}{2}, j, k\right)\right.$$
$$\left. + S_{\alpha h,y}^{n+\frac{1}{2}}\left(i+\frac{1}{2}, j, k\right) - S_{\alpha h,y}^n\left(i+\frac{1}{2}, j, k\right)\right]$$
$$+(\overline{\overline{\varepsilon^c}})_{13}^{-1}\left[D_z^{n+1}\left(i+\frac{1}{2}, j, k\right) - S_{e,z}^{n+\frac{1}{2}}\left(i+\frac{1}{2}, j, k\right)\right.$$
$$\left. + S_{\alpha h,z}^{n+\frac{1}{2}}\left(i+\frac{1}{2}, j, k\right) - S_{\alpha h,z}^n\left(i+\frac{1}{2}, j, k\right)\right] \tag{24.a}$$

$$\overline{\overline{\varepsilon}}(z) = \frac{1}{T}\overline{\overline{\varepsilon^c}} + \left[\left(\frac{(\varepsilon_s - \varepsilon_\infty)\omega_0}{\sqrt{1-\xi_0^2}}\right) \cdot \left(\frac{e^{-\omega_0 \xi_0 T} \cdot \sin\left(\omega_0 \sqrt{1-\xi_0^2}\, T\right) \cdot z^{-1}}{1 - 2e^{-\omega_0 \xi_0 T} \cdot \cos\left(\omega_0 \sqrt{1-\xi_0^2}\, T\right) \cdot z^{-1} + e^{-2\omega_0 \xi_0 T} \cdot z^{-2}}\overline{\overline{M}}_e\right)\right] \tag{17.a}$$

$$\overline{\overline{\mu}}(z) = \frac{1}{T}\overline{\overline{\mu^c}} + \left[\left(\frac{1-z^{-1}}{T}\right)^2 \left(\frac{(\mu_\infty - \mu_s)}{\omega_0 \sqrt{1-\xi_0^2}}\right)\right.$$
$$\left. \cdot \left(\frac{e^{-\omega_0 \xi_0 T} \cdot \sin\left(\omega_0 \sqrt{1-\xi_0^2}\, T\right) \cdot z^{-1}}{1 - 2e^{-\omega_0 \xi_0 T} \cdot \cos\left(\omega_0 \sqrt{1-\xi_0^2}\, T\right) \cdot z^{-1} + e^{-2\omega_0 \xi_0 T} \cdot z^{-2}}\overline{\overline{M}}_m\right)\right] \tag{17.b}$$

$$\overline{\overline{\alpha}}(z) = \left(\frac{1-z^{-1}}{T}\right) \cdot \left(\frac{\tau_\alpha \omega_0}{\sqrt{1-\xi_0^2}}\right)$$
$$\cdot \left(\frac{e^{-\omega_0 \xi_0 T} \sin\left(\omega_0 \sqrt{1-\xi_0^2}\, T\right) z^{-1}}{1 - 2e^{-\omega_0 \xi_0 T} \cos\left(\omega_0 \sqrt{1-\xi_0^2}\, T\right) z^{-1} + e^{-2\omega_0 \xi_0 T} z^{-2}}\overline{\overline{O}}\right). \tag{17.c}$$
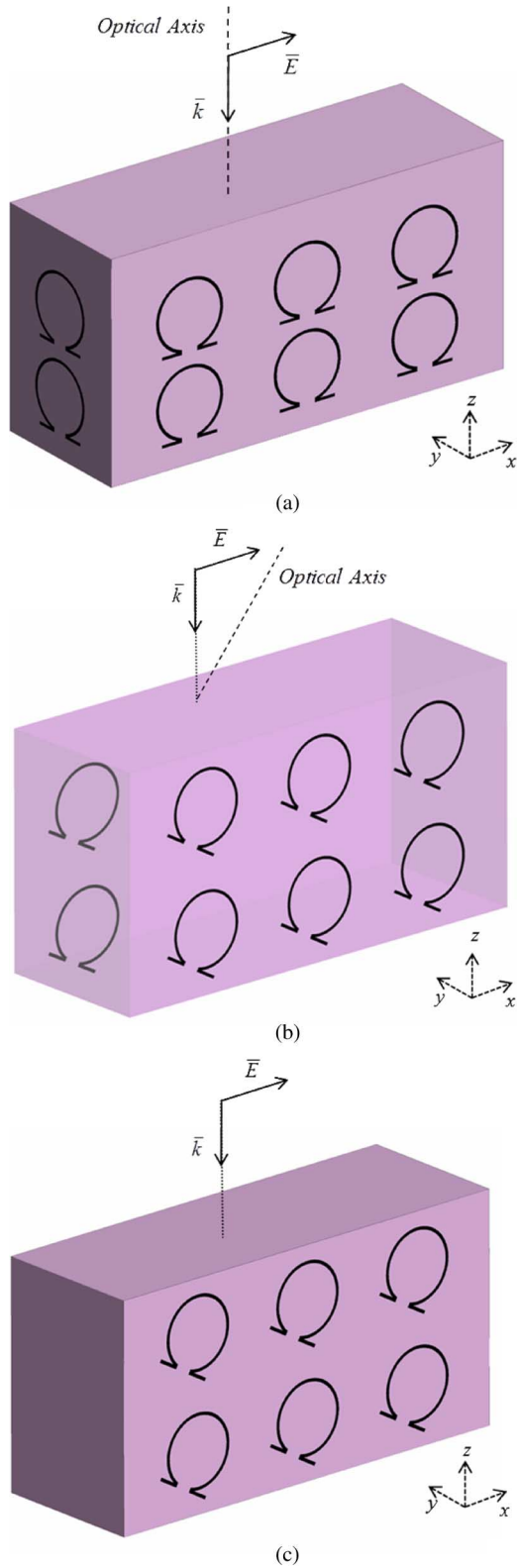
(a)

(b)

(c)

Fig. 2. Normal incidence of an x-polarized plane wave on a dispersive bian-isotropic slab. (a) Uniaxial omega slab. (b) Rotated uniaxial omega slab. (c) Rotated biaxial omega slab.

$$H_x^{n+1}\left(i,j+\frac{1}{2},k+\frac{1}{2}\right)$$
$$=+(\overline{\overline{\mu^c}})_{11}^{-1}\left[B_x^{n+1}\left(i,j+\frac{1}{2},k+\frac{1}{2}\right)\right.$$

$$-S_{h,x}^{n+\frac{1}{2}}\left(i,j+\frac{1}{2},k+\frac{1}{2}\right)$$
$$-S_{\alpha e,\tilde{x}}^{n+\frac{1}{2}}\left(i,j+\frac{1}{2},k+\frac{1}{2}\right)$$
$$\left.+S_{\alpha e,x}^{n}\left(i,j+\frac{1}{2},k+\frac{1}{2}\right)\right]$$
$$+(\overline{\overline{\mu^c}})_{12}^{-1}\left[B_y^{n+1}\left(i,j+\frac{1}{2},k+\frac{1}{2}\right)\right.$$
$$-S_{h,y}^{n+\frac{1}{2}}\left(i,j+\frac{1}{2},k+\frac{1}{2}\right)$$
$$-S_{\alpha e,\tilde{y}}^{n+\frac{1}{2}}\left(i,j+\frac{1}{2},k+\frac{1}{2}\right)$$
$$\left.+S_{\alpha e,y}^{n}\left(i,j+\frac{1}{2},k+\frac{1}{2}\right)\right]$$
$$+(\overline{\overline{\mu^c}})_{13}^{-1}\left[B_z^{n+1}\left(i,j+\frac{1}{2},k+\frac{1}{2}\right)\right.$$
$$-S_{h,z}^{n+\frac{1}{2}}\left(i,j+\frac{1}{2},k+\frac{1}{2}\right)$$
$$-S_{\alpha e,\tilde{z}}^{n+\frac{1}{2}}\left(i,j+\frac{1}{2},k+\frac{1}{2}\right)$$
$$\left.+S_{\alpha e,z}^{n}\left(i,j+\frac{1}{2},k+\frac{1}{2}\right)\right] \tag{24.b}$$

where $(\overline{\overline{\varepsilon^c}})_{ij}^{-1}$ and $(\overline{\overline{\mu^c}})_{ij}^{-1}$ are elements of inverse matrix of $\overline{\overline{\varepsilon^c}}$ and $\overline{\overline{\mu^c}}$, respectively, indexed by (i,j). The y and z components can be obtained similarly.

According to updating (23), new values of $\overline{E}$ and $\overline{H}$ depend on $\overline{D}$ and $\overline{B}$ calculated in the present time step and S vectors calculated in previous time steps. The values of flux density vectors $\overline{D}$ and $\overline{B}$ are given by (12) for the component x. However, the updating equations for S vectors are required. This is accomplished using (21). Vectors $\overline{S}_e$, $\overline{S}_h$, $\overline{S}_{\alpha e}$, and $\overline{S}_{\alpha h}$ are first written as

$$\overline{S}_e(z) = C_{\varepsilon 2}\overline{S}_e(z)z^{-1} - C_{\varepsilon 3}\overline{S}_e(z)z^{-2}$$
$$+ C_{\varepsilon 1}\overline{\overline{M}}_e.\overline{E}(z) \tag{25.a}$$
$$\overline{S}_h(z) = C_{\mu 2}\overline{S}_h(z)z^{-1} - C_{\mu 3}\overline{S}_h(z)z^{-2}$$
$$+ C_{\mu 1}\overline{\overline{M}}_m.\overline{H}(z) \tag{25.b}$$
$$\overline{S}_{\alpha e}(z) = C_{\alpha 2}\overline{S}_{\alpha e}(z)z^{-1} - C_{\alpha 3}\overline{S}_{\alpha e}(z)z^{-2}$$
$$+ C_{\alpha 1}\overline{\overline{O}}^t.\overline{E}(z) \tag{25.c}$$
$$\overline{S}_{\alpha h}(z) = C_{\alpha 2}\overline{S}_{\alpha h}(z)z^{-1} - C_{\alpha 3}\overline{S}_{\alpha h}(z)z^{-2}$$
$$+ C_{\alpha 1}\overline{\overline{O}}.\overline{H}(z). \tag{25.d}$$

By expressing the aforementioned equations in the discrete-time domain, updating equations for S vectors are simply obtained by

$$\overline{S}_e^{n+1} = C_{\varepsilon 2}\overline{S}_e^{n+\frac{1}{2}} - C_{\varepsilon 3}\overline{S}_e^n + C_{\varepsilon 1}\overline{\overline{M}}_e.\overline{E}^{n+1} \tag{26.a}$$
$$\overline{S}_h^{n+1} = C_{\mu 2}\overline{S}_h^{n+\frac{1}{2}} - C_{\mu 3}\overline{S}_h^n + C_{\mu 1}\overline{\overline{M}}_m.\overline{H}^{n+1} \tag{26.b}$$
$$\overline{S}_{\alpha e}^{n+1} = C_{\alpha 2}\overline{S}_{\alpha e}^{n+\frac{1}{2}} - C_{\alpha 3}\overline{S}_{\alpha e}^n + C_{\alpha 1}\overline{\overline{O}}^t.\overline{E}^{n+1} \tag{26.c}$$
$$\overline{S}_{\alpha h}^{n+1} = C_{\alpha 2}\overline{S}_{\alpha h}^{n+\frac{1}{2}} - C_{\alpha 3}\overline{S}_{\alpha h}^n + C_{\alpha 1}\overline{\overline{O}}.\overline{H}^{n+1}. \tag{26.d}$$
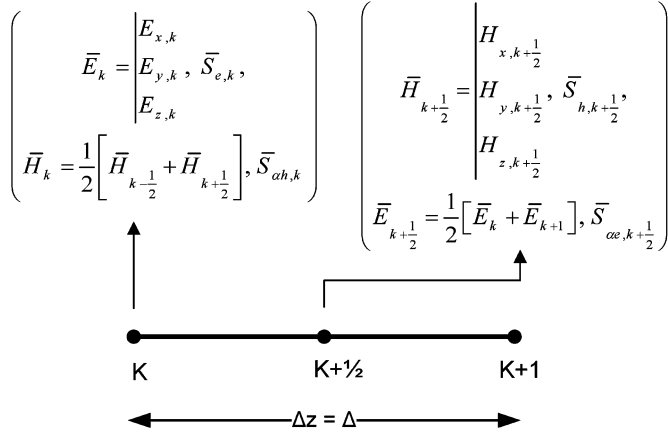
$$\left(\begin{array}{c} \bar{E}_k = \begin{vmatrix} E_{x,k} \\ E_{y,k} \\ E_{z,k} \end{vmatrix}, \bar{S}_{e,k}, \\ \bar{H}_k = \frac{1}{2}\left[\bar{H}_{k-\frac{1}{2}} + \bar{H}_{k+\frac{1}{2}} \right], \bar{S}_{\alpha h,k} \end{array} \right) \left(\begin{array}{c} \bar{H}_{k+\frac{1}{2}} = \begin{vmatrix} H_{x,k+\frac{1}{2}} \\ H_{y,k+\frac{1}{2}} \\ H_{z,k+\frac{1}{2}} \end{vmatrix}, \bar{S}_{h,k+\frac{1}{2}}, \\ \bar{E}_{k+\frac{1}{2}} = \frac{1}{2}\left[\bar{E}_k + \bar{E}_{k+1} \right], \bar{S}_{\alpha e,k+\frac{1}{2}} \end{array} \right)$$

K   K+½   K+1

$\Delta z = \Delta$

Fig. 3. 1-D FDTD cell used for modeling the bianisotropic media.

It should be noted that all of these equations must be decomposed into components x, y, and z in order to be used in FDTD formulation. For example, for the x components of S vectors, the following can be presented

$$S_{e,x}^{n+1} = C_{\varepsilon2}S_{e,x}^{n+\frac{1}{2}} - C_{\varepsilon3}S_{e,x}^n + C_{\varepsilon1} \\ \times \left(\mathrm{M}_{e,11}E_x^{n+1} + \mathrm{M}_{e,12}E_y^{n+1} + \mathrm{M}_{e,13}E_z^{n+1} \right) \quad (27.a)$$

$$S_{h,x}^{n+1} = C_{\mu2}S_{h,x}^{n+\frac{1}{2}} - C_{\mu3}S_{h,x}^n + C_{\mu1} \\ \times \left(\mathrm{M}_{m,11}\overline{H}_x^{n+1} + \mathrm{M}_{m,12}\overline{H}_y^{n+1} + \mathrm{M}_{m,13}\overline{H}_z^{n+1} \right) \quad (27.b)$$

$$S_{\alpha e,x}^{n+1} = C_{\alpha2}S_{\alpha e,x}^{n+\frac{1}{2}} - C_{\alpha3}S_{\alpha e,x}^n + C_{\alpha1} \\ \times \left(\mathrm{O}_{11}E_x^{n+1} + \mathrm{O}_{21}E_y^{n+1} + \mathrm{O}_{31}E_z^{n+1} \right) \quad (27.c)$$

$$S_{\alpha h,x}^{n+1} = C_{\alpha2}S_{\alpha h}^{n+\frac{1}{2}} - C_{\alpha3}S_{\alpha h}^n + C_{\alpha1} \\ \times \left(\mathrm{O}_{11}H_x^{n+1} + \mathrm{O}_{12}H_y^{n+1} + \mathrm{O}_{13}H_z^{n+1} \right). \quad (27.d)$$

According to (23) and (24), the vectors $\overline{S}_e$ and $\overline{S}_{\alpha h}$ must be calculated at points $(i, j, k + (1/2))$, $(i, j + (1/2), k)$, and $(i + (1/2), j, k)$. However, the vectors $\overline{S}_h$ and $\overline{S}_{\alpha e}$ must be evaluated at points $(i, j + (1/2), k + (1/2))$, $(i + (1/2), j, k + (1/2))$, and $(i + (1/2), j + (1/2), k)$. As a result, all components of the electric and magnetic fields must be known at different six points while in a conventional Yee's cell, each component of a field vector is defined only at one point. For instance, the x component of electric field is defined at $(i + (1/2), j, k)$. To overcome this problem, each component of the field is defined at five undefined points as the average of its values at neighboring defined points. The average formulas are given in the Appendix; for example, for the component x of the electric field.

At this point, the algorithm of FDTD is completed. The process of the FDTD in a dispersive bianisotropic medium is carried out in the following order:

1. Updating all components of flux vectors [using (12)];
2. Updating all components of field vectors [using (24)];
3. Defining all components of electric and magnetic field vectors at undefined points as the average of their values at neighboring defined points (see Appendix);
4. Updating all components of S vectors [using (27)].

In the next part of the paper, this algorithm is applied to the problem of normal incidence of electromagnetic waves, on an omega slab in several cases of arrangement of Ω-shaped particles in the slab.

III. FDTD SIMULATION OF NORMAL INCIDENCE ON A SLAB OF BIANISOTROPIC MEDIUM

In this section, the presented formulation is used to simulate plane wave normal incidence on a dispersive bianisotropic slab in three different cases illustrated in Fig. 2. First, the slab is assumed to be a uniaxial medium where the optical axis is along the propagation vector [Fig. 2(a)]. Second, a rotated slab of uniaxial medium where the optical axis is not along propagation vector is considered [Fig. 2(b)]. Third, a slab of rotated biaxial medium is simulated [Fig. 2(c)]. As a numerical example in our simulations, a slab of omega medium is considered through the following parameters

$$\varepsilon_\infty = 2, \ \varepsilon_s = 5, \ \varepsilon_n = 1.5, \\ \mu_\infty = 1.1, \ \mu_s = 1.8, \ \mu_{n=1}, \\ f_0 = \frac{\omega_0}{2\pi} = 2 \text{ GHz}, \ \xi_0 = 0.5, \ \tau_K = \frac{0.7}{\omega_0}. \quad (28)$$

It is noted that with these values, constitutive tensors obey the conditions for constitutive tensors of lossy bianisotropic media, given in [40].

The thickness of the slab is assumed to be 10 cm (in the z direction). The 1-D FDTD computational space is 1 meter long which consists of 1000 cells where the slab is assumed to be located between cells 450 and 550 in the middle of computational space. A schematic of 1-D FDTD cell is presented in Fig. 3. As noted in Section II, attendance of each component of the electric and magnetic fields is necessary for FDTD modeling of Bianisotropic media. The soft lattice truncation conditions [41] are applied on both sides of computation space. Because of dispersion and bianisotropy of the medium, the time step should be chosen short enough to avoid the instability of FDTD method. Hence, in this paper, the time step δt is set to $\delta t = \Delta/20c_0 = (d/100)/20c_0$, where Δ is the length of cells, d is the slab thickness, and c_0 is light velocity in free space. The choice of very small δt is due to the special frequency dispersion model (6.b). In FDTD simulations, the slab is illuminated by an x-polarized Gaussian waveform of electromagnetic plane wave propagating along $\hat{z}$. It is desired to transform time-domain results of FDTD to frequency domain and calculate the transmission and reflection coefficients. Discrete Fourier transform (DFT) is used to obtain frequency-domain data. The results of FDTD method are compared with the exact results, calculated based on the analytical method presented in [36]. The comparison of results illustrates the high accuracy of the presented FDTD method.

A. Normal Incidence on a Uniaxial Omega Slab, Propagation Along the Optical Axis

In the first example, a slab of uniaxial omega medium with an optical axis along $\hat{z}$ is assumed which is illuminated by an x-polarized plane wave propagating in the $\hat{z}$ direction [Fig. 2(a)]. The constitutive relations of medium are given in (5.a) and (5.b) and
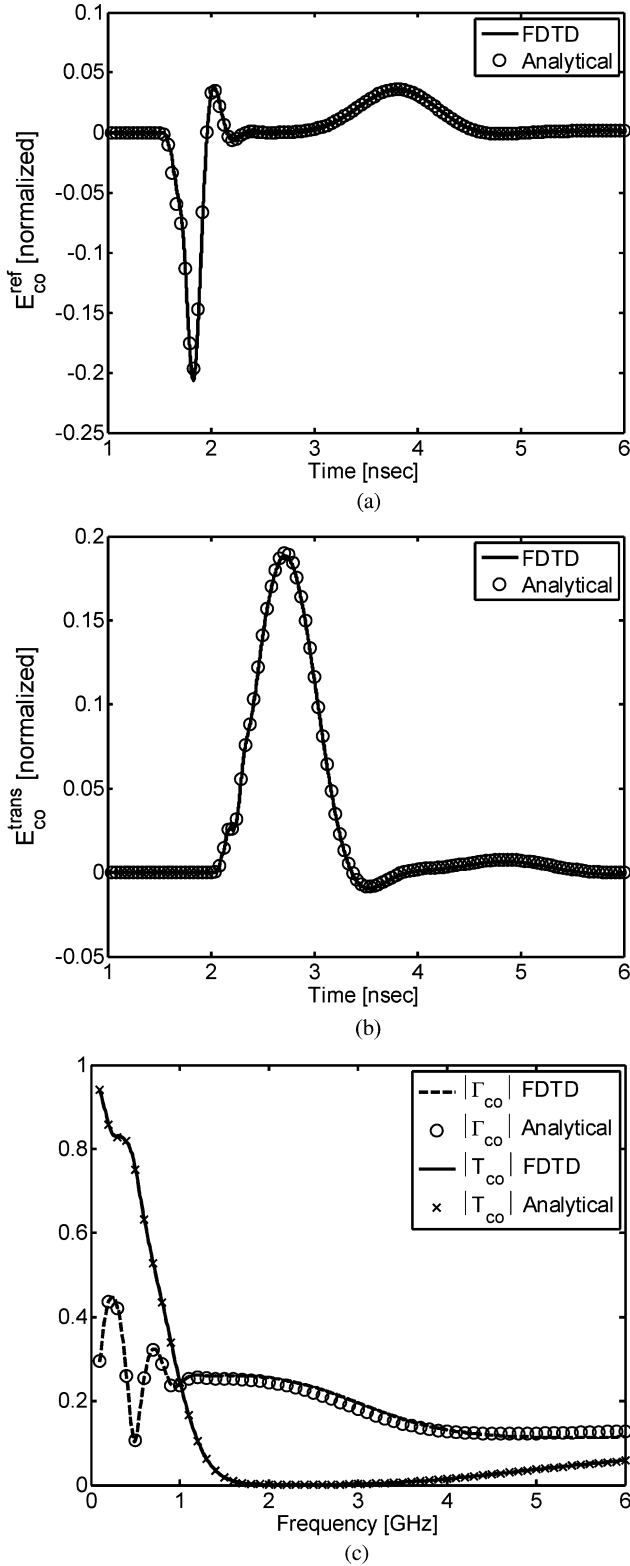
Fig. 4. Simulation results of normal incidence of a Gaussian plane wave on uniaxial omega slab along its optical axis. (a) Co-polarized reflected field in time domain. (b) Co-polarized transmitted field in time domain. (c) Co-polarization of reflection and transmission coefficients in frequency domain.

constitutive tensors and their components are given in (6) and (28).

From (3), the bianisotropy of the medium couples the x and y components of electric field to the y and x components of the magnetic field, respectively. As the incident wave consists of x and y components of electric and magnetic fields, respectively, other components of fields, component y of the electric field and component x of the magnetic field, do not appear. Hence, the cross-polarizations of reflected and transmitted waves do not exist. The FDTD simulation agrees with this statement and cross-polarized reflection and transmission coefficients are zero. In Fig. 4, the co-polarizations of FDTD simulation results are shown and compared with analytical results. The comparison shows a good agreement between the developed FDTD results and analytic solutions. Time-domain reflected and transmitted waves are presented in Fig. 4(a) and Fig. 4(b), respectively, and frequency-domain reflection and transmission coefficients are demonstrated in Fig. 4(c).

B. Normal Incidence on Rotated Uniaxial Omega Slab

In the second example, a normally incident x-polarized plane wave propagating along the $\hat{z}$ direction illuminates a slab of uniaxial omega medium with its optical axis not parallel to the propagation vector [Fig. 2(b)]. For this case, rotated Ω particles are assumed in the slab. For instance, the Euler angles are set to $\alpha = 10°$, $\beta = 15°$, and $\gamma = 45°$. The constitutive tensors of the rotated medium are given by (9) and the parameters are determined by (6) and (28).

Due to the effect of rotation matrix U in (9.c), the magneto-electric coupling tensor $\overline{\overline{\alpha}}$ becomes a dense matrix with many non-zero elements, resulting in a relatively strong magnetoelectric coupling between all the components of electric and magnetic fields. Here, all components of electric and magnetic fields appear in the slab. Due to the anisotropy of the medium, $\nabla.\overline{E} \neq 0$ and $\nabla.\overline{H} \neq 0$. Therefore, the z components of the fields may exist in the slab and propagate along the $\hat{z}$ direction. However, these components vanish at the slab boundaries and do not propagate outside the slab. In this example, the reflected and transmitted waves have both co- and cross-polarizations illustrated in Fig. 5 and Fig. 6, respectively. The FDTD results and related analytical solutions are compared. They reveal a good accuracy of the developed FDTD method for the dispersive bianisotropic media.

C. Incidence on Rotated Biaxial Omega Slab

In the final example, a normal incidence of plane wave on a slab of rotated biaxial omega medium is considered [Fig. 2(c)]. In this case, constitutive relations are given in (10) and parameters are defined as the previous example. Because of rotation, as in the last example, $\overline{\overline{\alpha}}$ is a dense matrix. Therefore, co- and cross-polarizations of transmitted and reflected waves both exist. The results of FDTD simulation and comparison with the exact solution are provided in Fig. 7 and Fig. 8 for co- and cross-polarizations, respectively.

IV. CONCLUSION

In this paper, the FDTD method is developed for simulating the electromagnetic wave interaction with dispersive bianisotropic media. The Z-transform method is used in developing
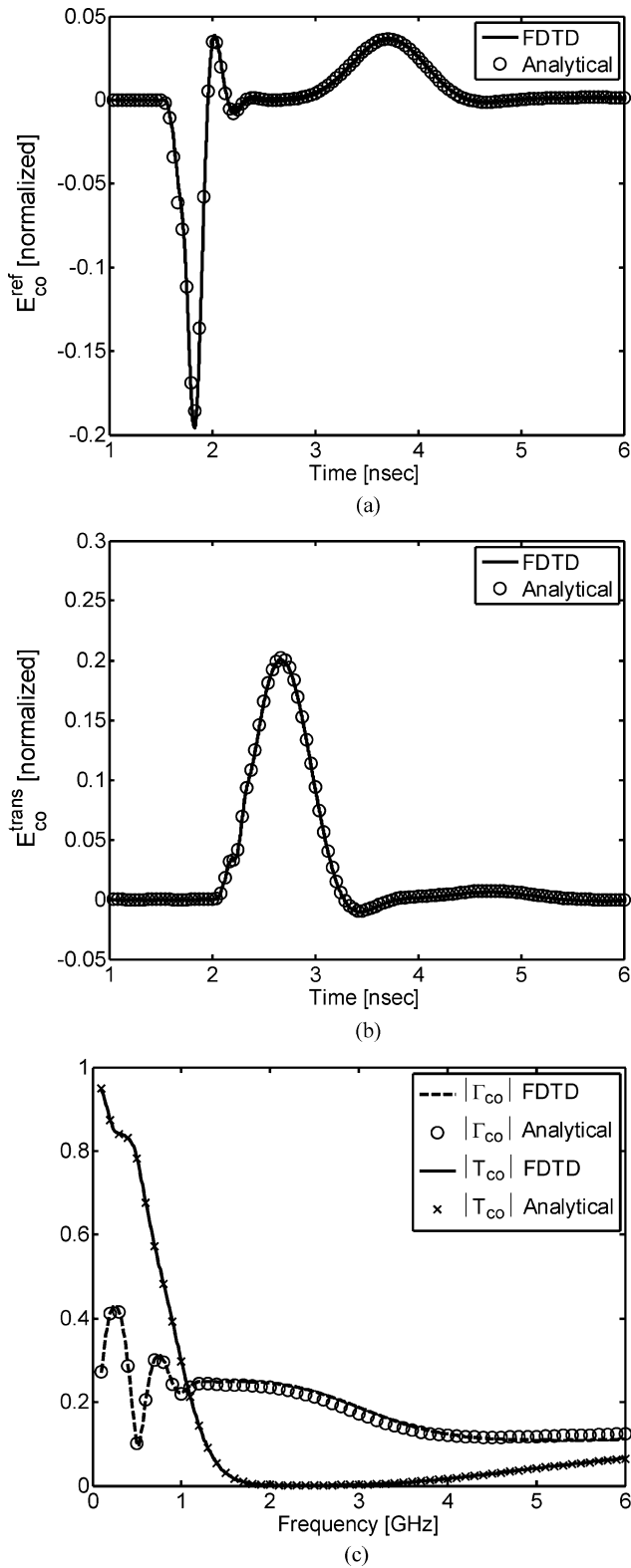
Fig. 5. Simulation results of co-polarized (a) reflected field. (b) Transmitted field in time domain. (c) Reflection and transmission coefficients in frequency domain of a rotated uniaxial omega slab illuminated by normal incidence of a Gaussian plane wave.
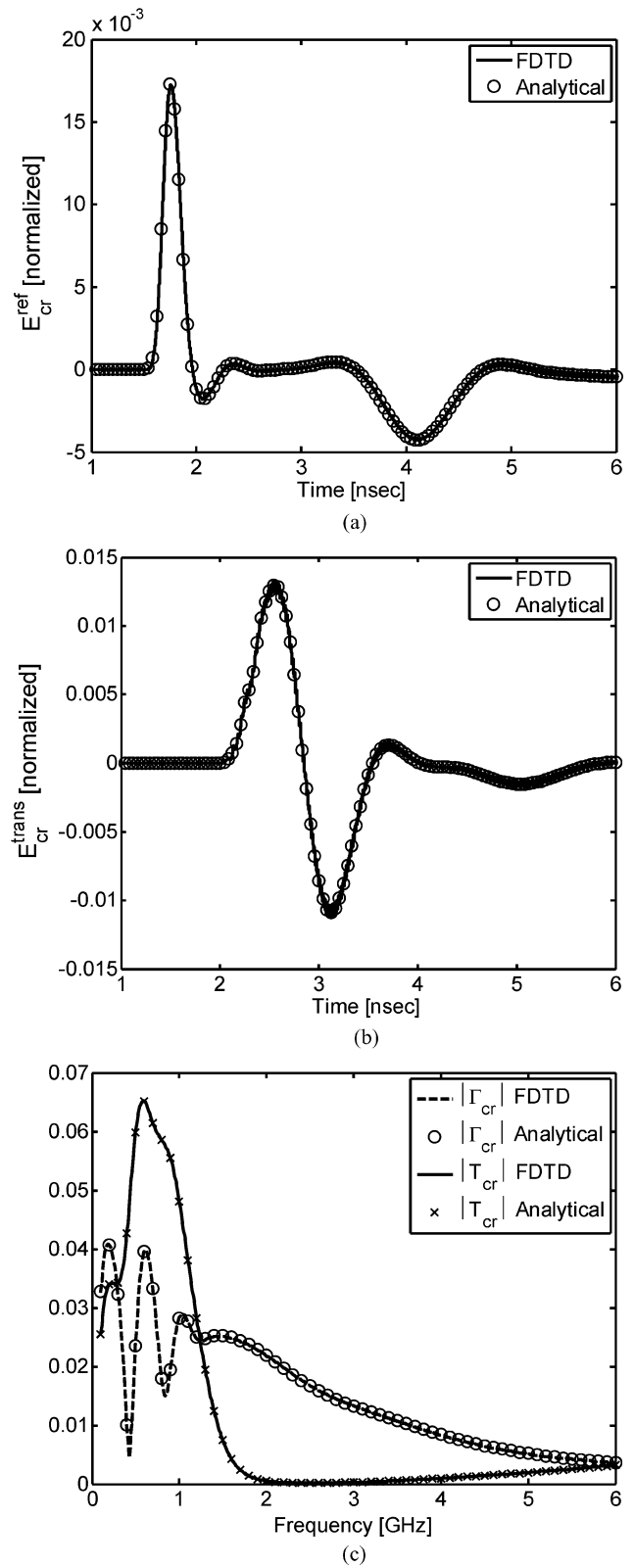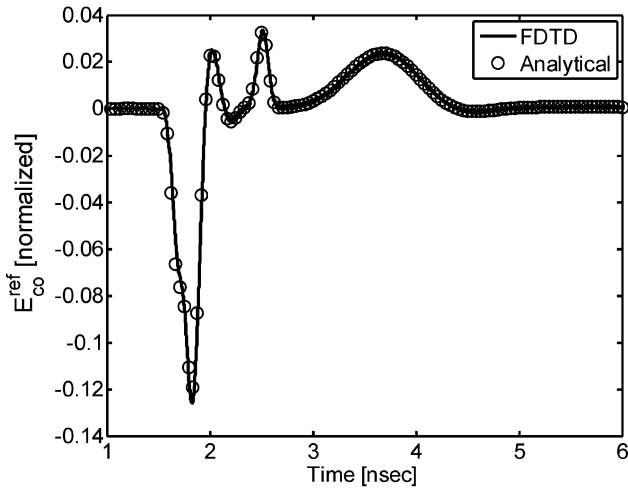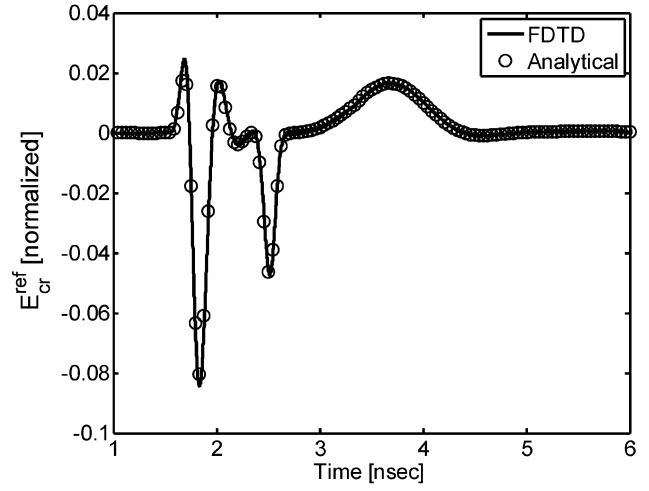

Fig. 6. Simulation results of cross-polarized (a) reflected field. (b) Transmitted field in time domain. (c) Reflection and transmission coefficients in frequency domain of a rotated uniaxial omega slab illuminated by normal incidence of a Gaussian plane wave.

the technique. Due to anisotropy of media, tensor notation is used in the formulation of FDTD. The developed FDTD method is applied to simulate the interaction of electromagnetic plane

waves with both uniaxial and biaxial omega media in order to extract co- and cross-polarized, transmitted and reflected waves
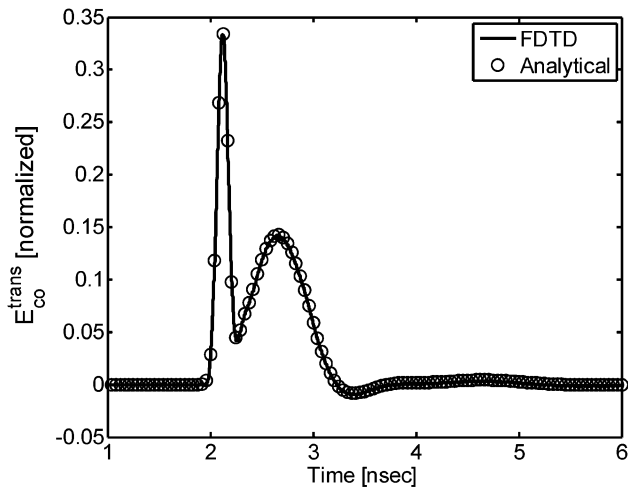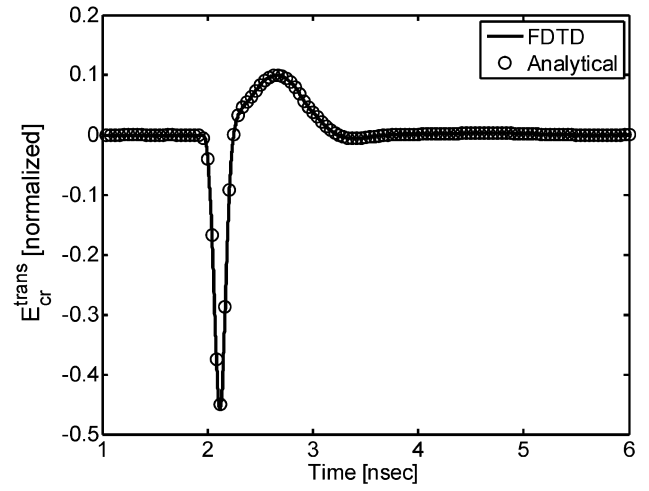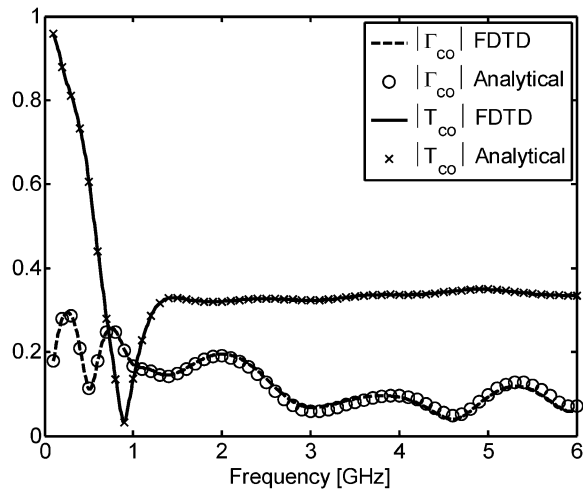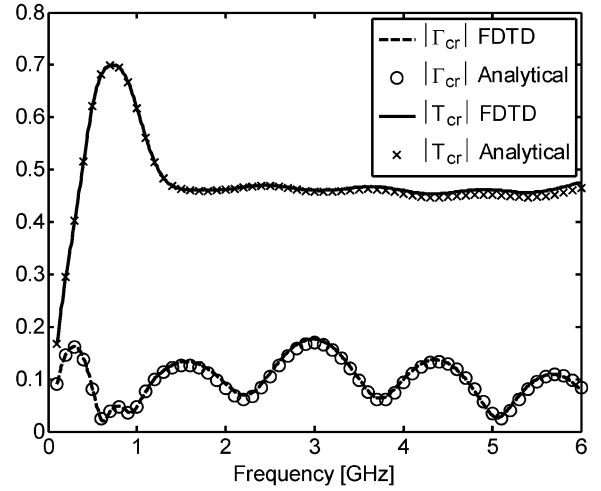
Fig. 7. Simulation results of co-polarized (a) reflected field. (b) Transmitted field in time domain. (c) Reflection and transmission coefficients in frequency domain of a rotated biaxial omega slab illuminated by normal incidence of a Gaussian plane wave.

Fig. 8. Simulation results of cross-polarized (a) reflected field. (b) Transmitted field in time domain. (c) Reflection and transmission coefficients in frequency domain of a rotated biaxial omega slab illuminated by normal incidence of a Gaussian plane wave.

in time domain and reflection and transmission coefficients in frequency domain. The numerical results of FDTD are compared with analytical results and a good agreement is observed.

APPENDIX

The component x of electric field at points $(i, j, k + (1/2))$, $(i, j + (1/2), k)$, $(i, j + (1/2), k + (1/2))$, $(i + (1/2), j, k +$

$(1/2))$, and $(i+(1/2), j+(1/2), k)$ is not defined in a Yee cell. To define this component of the field, the same component of the field at the neighbors is averaged as follows:

$$
E_x\left(i, j+\frac{1}{2}, k\right)
$$
$$
= \frac{1}{4}\left[E_x\left(i-\frac{1}{2}, j, k\right) + E_x\left(i-\frac{1}{2}, j+1, k\right)\right.
$$
$$
\left. + E_x\left(i+\frac{1}{2}, j+1, k\right) + E_x\left(i+\frac{1}{2}, j, k\right)\right] \quad \text{(A.1)}
$$

$$
E_x\left(i, j, k+\frac{1}{2}\right)
$$
$$
= \frac{1}{4}\left[E_x\left(i+\frac{1}{2}, j, k\right) + E_x\left(i+\frac{1}{2}, j, k+1\right)\right.
$$
$$
\left. + E_x\left(i-\frac{1}{2}, j, k\right) + E_x\left(i-\frac{1}{2}, j, k+1\right)\right] \quad \text{(A.2)}
$$

$$
E_x\left(i, j+\frac{1}{2}, k+\frac{1}{2}\right)
$$
$$
= \frac{1}{8}\left[E_x\left(i-\frac{1}{2}, j, k\right) + E_x\left(i+\frac{1}{2}, j, k\right)\right.
$$
$$
+ E_x\left(i-\frac{1}{2}, j+1, k\right) + E_x\left(i+\frac{1}{2}, j+1, k\right)
$$
$$
+ E_x\left(i+\frac{1}{2}, j, k+1\right) + E_x\left(i+\frac{1}{2}, j+1, k+1\right)
$$
$$
+ E_x\left(i-\frac{1}{2}, j, k+1\right)
$$
$$
\left. + E_x\left(i-\frac{1}{2}, j+1, k+1\right)\right] \quad \text{(A.3)}
$$

$$
E_x\left(i+\frac{1}{2}, j, k+\frac{1}{2}\right)
$$
$$
= \frac{1}{2}\left[E_x\left(i+\frac{1}{2}, j, k\right) + E_x\left(i+\frac{1}{2}, j, k+1\right)\right] \quad \text{(A.4)}
$$

$$
E_x\left(i+\frac{1}{2}, j+\frac{1}{2}, k\right)
$$
$$
= \frac{1}{2}\left[E_x\left(i+\frac{1}{2}, j, k\right) + E_x\left(i+\frac{1}{2}, j+1, k\right)\right]. \quad \text{(A.5)}
$$

Other components of E and H fields are averaged in a similar manner.

ACKNOWLEDGMENT

REFERENCES

[1] S. A. Tretyakov and A. A. Sochava, "Proposed composite material for nonreflecting shields and antenna radomes," *IET Electron. Lett.*, vol. 29, no. 12, p. 1048, 1993.

[2] S. A. Tretyakov and A. A. Sihvola, "Novel uniaxial bianisotropic materials: Reflection and transmission in planar structures," *Progress in Electromagn. Res.*, vol. 9, pp. 157–179, 1994.

[3] R. Yang, Y. Xie, and X. Li *et al.*, "Slow wave propagation in nonradiative dielectric waveguides with bianisotropic split ring resonator metamaterials," *Infrared Phys. Technol.*, vol. 51, no. 6, pp. 555–558, 2008.

[4] V. Butylkin and G. Kraftmakher, "Passbands of bianisotropic and waveguide bianisotropic metamaterials based on planar double split rings," *J. Commun. Technol. Electron.*, vol. 53, no. 1, pp. 1–14, 2008.

[5] V. S. Butylkin and G. A. Kraftmakher, "Nonreciprocal effects in propagation of microwaves along a waveguide structure formed from a ferrite plate and a lattice of resonant elements," *J. Commun. Technol. Electron.*, vol. 54, no. 7, pp. 775–782, 2009.

[6] S. L. Prosvirnin and N. I. Zheludev, "Analysis of polarization transformations by a planar chiral array of complex-shaped particles," *J. Opt. A: Pure and Appl. Opt.*, vol. 11, no. 7, p. 074002, 2009.

[7] P. Pelet and N. Engheta, "Novel rotational characteristics of radiation patterns of chirostrip dipole antennas," *Microw. Opt. Technol. Lett.*, vol. 5, no. 1, pp. 31–34, 1992.

[8] P. Pelet and N. Engheta, "Mutual coupling in finite-length thin wire chirostrip antennas," *Microw. Opt. Technol. Lett.*, vol. 6, no. 12, pp. 671–675, 1993.

[9] P. Kalaee and J. Rashed-Mohassel, "Investigation of dipole radiation pattern above a chiral media using 3D BI-FDTD approach," *J. Electromagn. Waves Appl.*, vol. 23, no. 1, pp. 75–86, 2009.

[10] Z. Chemseddine and B. Fatiha, "Asymptotic approach for rectangular microstrip patch antenna with magnetic anisotropy and chiral substrate," *Int. J. Electron., Circuits Syst.*, vol. 3, no. 2, pp. 84–90, 2009.

[11] N. Landy, C. Bingham, and T. Tyler *et al.*, "Design, theory, and measurement of a polarization-insensitive absorber for terahertz imaging," *Phys. Rev. B*, vol. 79, no. 12, 2009.

[12] H. Tao, A. Strikwerda, and K. Fan *et al.*, "Reconfigurable terahertz metamaterials," *Phy. Rev. Lett.*, vol. 103, no. 14, p. 147401, 2009.

[13] S. A. Tretyakov, C. R. Simovski, and M. Hudlička, "Bianisotropic route to the realization and matching of backward-wave metamaterial slabs," *Phys. Rev. B*, vol. 75, no. 15, p. 153104, 2007.

[14] K. Guven, E. Saenz, and R. Gonzalo *et al.*, "Electromagnetic cloaking with canonical spiral inclusions," *New J. Phys.*, vol. 10, no. 11, p. 115037, 2008.

[15] F. Hunsberger, R. Luebbers, and K. Kunz, "Finite-difference time-domain analysis of gyrotropic media. I. Magnetized plasma," *IEEE Trans. Antennas Propag.*, vol. 40, no. 12, pp. 1489–1495, 1992.

[16] S. Gonzalez Garcia, I. Villo Perez, and R. G. Martin *et al.*, "Extension of Berenger's PML for bi-isotropic media," *IEEE Microw. Guided Wave Lett.*, vol. 8, no. 9, pp. 297–299, 1998.

[17] S. G. Garcia, I. V. Perez, and R. G. Martin *et al.*, "BiPML: A PML to match waves in bi-anisotropic media," *Microw. Opt. Technol. Lett.*, vol. 20, no. 1, pp. 44–48, 1999.

[18] F. Ji, E. K. N. Yung, and X. Q. Sheng, "Three-dimensional FDTD analysis of chiral discontinuities in the waveguide," *Int. J. Infrared Millimeter Waves*, vol. 23, no. 10, pp. 1521–1528, 2002.

[19] A. Akyurtlu, D. H. Werner, and K. Aydin, "BI-FDTD: A new technique for modeling electromagnetic wave interaction with bi-isotropic media," *Microw. Opt. Technol. Lett.*, vol. 26, no. 4, pp. 239–242, 2000.

[20] A. Akyurtlu and D. H. Werner, "BI-FDTD: A novel finite-difference time-domain formulation for modeling wave propagation in bi-isotropic media," *IEEE Trans. Antennas Propag.*, vol. 52, no. 2, pp. 416–425, 2004.

[21] A. Grande, I. Barba, and A. C. L. Cabeceira *et al.*, "FDTD modeling of transient microwave signals in dispersive and lossy bi-isotropic media," *IEEE Trans. Microw. Theory Techn.*, vol. 52, no. 3, pp. 773–784, 2004.

[22] V. Demir, A. Z. Elsherbeni, and E. Arvas, "FDTD formulation for dispersive chiral media using the Z transform method," *IEEE Trans. Antennas Propag.*, vol. 53, no. 10, pp. 3374–3384, 2005.

[23] A. Semichaevsky and A. Akyurtlu, "A new uniaxial perfectly matched layer absorbing boundary condition for chiral metamaterials," *IEEE Antennas Wireless Propag. Lett.*, vol. 4, pp. 51–54, 2005.

[24] A. Semichaevsky, A. Akyurtlu, and D. Kern *et al.*, "Novel BI-FDTD approach for the analysis of chiral cylinders and spheres," *IEEE Trans. Antennas Propag.*, vol. 54, no. 3, pp. 925–932, 2006.

[25] J. A. Pereda, A. Grande, and O. Gonzalez *et al.*, "FDTD modeling of chiral media by using the Mobius transformation technique," *IEEE Antennas Wireless Propag. Lett.*, vol. 5, no. 1, pp. 327–330, 2006.

[26] C. Hulse and A. Knoesen, "Dispersive models for the finite-difference time-domain method: Design, analysis, and implementation," *J. Opt. Soc. Amer. A*, vol. 11, no. 6, pp. 1802–1811, 1994.

[27] J. L. Young and R. O. Nelson, "A summary and systematic analysis of FDTD algorithms for linearly dispersive media," *IEEE Antennas Propag. Mag.*, vol. 43, no. 1, pp. 61–126, 2001.

[28] R. Siushansian and J. LoVetri, "A comparison of numerical techniques for modeling electromagnetic dispersive media," *IEEE Microw. Guided Wave Lett.*, vol. 5, no. 12, pp. 426–428, 1995.

[29] L. Zhili and L. Thylen, "On the accuracy and stability of several widely used FDTD approaches for modeling Lorentz dielectrics," *IEEE Trans. Antennas Propag.*, vol. 57, no. 10, pp. 3378–3381, 2009.

[30] J. A. Pereda, A. Vegas, and A. Prieto, "FDTD modeling of wave propagation in dispersive media by using the Mobius transformation technique," *IEEE Trans. Microwave Theory Techn.*, vol. 50, no. 7, pp. 1689–1695, 2002.

[31] A. Akyurtlu and D. H. Werner, "Modeling of transverse propagation through a uniaxial bianisotropic medium using the finite-difference time-domain technique," *IEEE Trans. Antennas Propag.*, vol. 52, no. 12, pp. 3273–3279, 2004.

[32] M. M. I. Saadoun and N. Engheta, "A reciprocal phase shifter using novel pseudochiral or ω medium," *Microw. Opt. Technol. Lett.*, vol. 5, no. 4, pp. 184–188, 1992.

[33] C. R. Simovski, S. A. Tretyakov, and A. A. Sochava *et al.*, "Antenna model for conductive omega particles," *J. Electromagn. Waves Appl.*, vol. 11, no. 1, pp. 1509–1530, 1997.

[34] A. Serdyukov, I. Semchenko, and S. A. Tretyakov *et al.*, *Electromagnetics of Bi-Anisotropic Materials, Theory and Applications*. New York: Gordon and Breach, 2001.

[35] T. G. Kharina, S. A. Tretyakov, and A. A. Sochava *et al.*, "Experimental studies of artificial omega media," *Electromagn.*, vol. 18, no. 4, pp. 423–437, 1998.

[36] S. Rikte, G. Kristensson, and M. Andersson, "Propagation in bianisotropic media—Reflection and transmission," *IEE Proc. Microw., Antennas Propag.*, vol. 148, no. 1, pp. 29–36, 2001.

[37] S. Zouhdi, A. A. Sihvola, and M. Arsalane, *Advances in Electromagnetics of Complex Media and Metamaterials*. Amsterdam, Netherlands: Kluwer Academic , 2002.

[38] L. Tsang, J. A. Kong, and K. H. Ding, *Scattering of Electromagnetic Waves: Theories and Applications*. New York: Wiley, 2000.

[39] D. M. Sullivan, "Frequency-dependent FDTD methods using Z transforms," *IEEE Trans. Antennas Propag.*, vol. 40, no. 10, pp. 1223–1230, 1992.

[40] I. V. Lindell, A. H. Sihvola, and P. Puska *et al.*, "Conditions for the parameter dyadics of lossless bianisotropic media," *Microw. Opt. Technol. Lett.*, vol. 8, no. 5, pp. 268–272, 1995.

[41] A. Taflove and M. E. Brodwin, "Numerical solution of steady-state electromagnetic scattering problems using the time-dependent Maxwell's equations," *IEEE Trans. Microw. Theory Techn.*, vol. 23, no. 8, pp. 623–630, 1975.

Mohammad Soleimani received the B.S. degree in electrical engineering from the University of Shiraz, Shiraz, Iran, in 1978 and the M.S. and Ph.D. degrees from Pierre and Marie Curio University, Paris, France, in 1981 and 1983, respectively.

He is working as a Professor with the Iran University of Sciences and Technology, Tehran, Iran. His research interests are in antennas, small satellites, electromagnetics, and radars. He has served in many executive and research positions including: Minister of ICT, Student Deputy of Ministry of Science, Research and Technology, Head of Iran Research Organization for Science and Technology, Head of Center for Advanced Electronics Research Center; and Technology Director for Space Systems in Iran Telecommunication Industries.
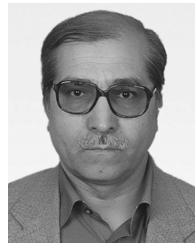
Jalil Rashed-Mohassel (SM'07) received the M.Sc. degree in electronics engineering from the University of Tehran, Tehran, Iran, in 1976 and the Ph.D. degree in electrical engineering from the University of Michigan, Ann Arbor, in 1982.

Formerly, he was with the University of Sistan and Baluchestan, Zahedan, Iran, where he held several academic and administrative positions. In 1994, he joined the University of Tehran where he is doing teaching and research as a Professor in antennas, EM theory, and applied mathematics.

Dr. Rashed-Mohassel served as the academic Vice-Dean, College of Engineering, General Director of Academic Affairs, University of Tehran, and is currently Chairman of the ECE Department, Principal Member of Center of Excellence on Applied Electromagnetic Systems, and the Director of the Microwave Laboratory. He was selected as the Brilliant National Researcher by the Iranian Association of Electrical and Electronics Engineers in 2007, and was the Distinguished Professor (2008–2009) in the 1st Education Festival, University of Tehran.

Vahid Nayyeri (S'08) was born in Tehran, Iran, in 1983. He received the B.S. degree from the Iran University of Science and Technology (IUST), Tehran, in 2006 and the M.S. degree from the University of Teheran, in 2008, both in electrical engineering.

Since 2008, he has been working toward the Ph.D. degree in electrical engineering at the IUST. His research interests include finite-difference time-domain method, electromagnetics of complex media, numerical analysis of electromagnetic wave interaction with them, and optimization methods in electromagnetic problems.

Mojtaba Dehmollaian was born in Iran in 1978. He received the B.S. and M.S. degrees in electrical engineering from the University of Tehran, Tehran, Iran, in 2000 and 2002, respectively. He received the M.S. degree in applied mathematics and the Ph.D. degree in electrical engineering from the University of Michigan, Ann Arbor, in 2007.

Currently, he is an Assistant Professor with the Department of Electrical and Computer Engineering, University of Tehran. His research interests are applied electromagnetics, radar remote sensing, and electromagnetic wave propagation, and scattering.

Dr. Dehmollaian was the recipient of the IEEE Geoscience and Remote Sensing Symposium (IGARSS) 2007 Prize Paper award.